Evaluation of Pediatric CNS Malignancies with ^{99m}Tc-Methoxyisobutylisonitrile SPECT

Adam Kirton, MD, MSc[1]; Reinhard Kloiber, MD[2]; Jane Rigel[3]; and Johannes Wolff, MD[3]

[1]Department of Pediatrics, Alberta Children's Hospital, University of Calgary, Calgary, Alberta, Canada; [2]Department of Nuclear Medicine, Alberta Children's Hospital, University of Calgary, Calgary, Alberta, Canada; and [3]Department of Pediatric Oncology, Alberta Children's Hospital, University of Calgary, Calgary, Alberta, Canada

SPECT has the potential to add valuable information to the diagnosis and management of central nervous system (CNS) malignancy. Radioactive tracers including ^{99m}Tc-methoxyisobutylisonitrile (MIBI), or sestamibi, have been shown to be sensitive markers for brain tumors; however, their role in imaging children is poorly defined. **Methods:** We undertook a pilot study of 29 pairs of ^{99m}Tc-MIBI and MRI images from 20 children to explore the clinical usefulness of this tracer in CNS malignancy. **Results:** Tumor types that took up ^{99m}Tc-MIBI included brain stem glioma, fibrillary astrocytoma, other low-grade astrocytomas, and glioblastoma multiforme. Most tumors positive for ^{99m}Tc-MIBI uptake were astrocytomas, including those in the brain stem, cerebellum, and cortex. This method of nuclear imaging not only was able to identify the presence of a tumor but also could identify changes in the same tumor over time. Some correlation between histologic grade and ^{99m}Tc-MIBI uptake was observed. Several tumors, including craniopharyngioma, medulloblastoma, and optic glioma, were evident on MRI but not on ^{99m}Tc-MIBI SPECT. **Conclusion:** The results suggest that this modality is a potentially useful tool in the diagnosis and management of CNS malignancies, particularly higher-grade astrocytomas, in children.

Key Words: sestamibi; brain tumor; child; SPECT

J Nucl Med 2002; 43:1438–1443

Accurate neuroimaging can assist in the diagnosis, management, prognosis, and follow-up of central nervous system (CNS) malignancies in children. SPECT has been established as a potentially useful tool for the assessment of brain tumors (*1–7*). In adults with gliomas, SPECT using ^{201}Tl has been applied to help differentiate between residual tumor and radiation necrosis (*8*) and predict the histologic grade (*6*)—information not easily attainable by MRI alone. Although some studies have suggested a similar usefulness for thallium SPECT in childhood brain tumors (*9*), other prospective studies have failed to demonstrate any clinical advantage over MRI (*10*).

Received Dec. 10, 2001; revision accepted Jul. 10, 2002.

For correspondence or reprints contact: Adam Kirton, MD, MSc, Department of Pediatrics, Alberta Children's Hospital, 1820 Richmond Rd. SW, Calgary, Alberta T2T 5C7, Canada.

E-mail: adamkirton@hotmail.com

^{99m}Tc-methoxyisobutylisonitrile (MIBI), or sestamibi, has been suggested to offer advantages over thallium for imaging of brain tumors (*11*). This molecule does not penetrate the intact blood–brain barrier. It is taken up by normal choroid plexus, pituitary, scalp, and nasopharyngeal tissues (*2,11–13*).

^{99m}Tc-MIBI uptake by viable tumor cells and brain malignancies is well established (*2,9,14–16*). Carcinoma cell lines accumulate 9 times more ^{99m}Tc-MIBI than do normal cell lines (*17*), and it is concentrated by numerous other human neoplasms (*18,19*). Human brain malignancies shown to accumulate ^{99m}Tc-MIBI include astrocytoma (*11,20*), acoustic schwannoma (*13,21*), CNS lymphoma (*20*), meningioma (*11,13,22*), metastatic brain tumors (*23*), and choroid plexus carcinoma (*14*).

^{99m}Tc-MIBI SPECT can add valuable information to CT for the differentiation of radiation necrosis from recurrent disease in adult brain malignancy (*24*). Despite the potential advantages and some experience with ^{99m}Tc-MIBI SPECT in children, a clear advantage over other modalities, including ^{201}Tl SPECT, in imaging brain tumors has not been established (*2,9,25,26*).

We undertook a pilot study of 20 children with a variety of brain tumors to investigate the clinical utility of ^{99m}Tc-MIBI imaging in comparison with standard MRI methods. Our results provided evidence from a group of pediatric patients that this modality may be a potentially useful tool in the diagnosis, management, and follow-up of specific CNS malignancies of childhood.

MATERIALS AND METHODS

Patients

SPECT with ^{99m}Tc-MIBI and gadolinium-enhanced MRI were completed on 20 children with CNS malignancy. Informed consent was obtained from all parents or legal guardians. The study was approved by the ethics review committee at the Alberta Children's Hospital. All eligible patients were sequentially enrolled and followed through the Southern Alberta Cancer Clinic and imaged between 1997 and 2000. Diagnoses were confirmed histologically with the exception of 4 brain stem gliomas, for which diagnosis was made radiologically. The longest time between MRI and ^{99m}Tc-MIBI imaging was 2 wk (1 patient), with the majority of study pairings being completed either the same day or within 72 h

TABLE 1
Patient Profiles, Tumor Type, and Location

Patient no.	Age (y)	Sex	Tumor	Location
1	6	M	Brain stem glioma	Midbrain
2	9	F	Brain stem glioma	Midbrain
3	15	M	Brain stem glioma	Midbrain
4	8	M	Brain stem glioma	Midbrain
5	5	M	Brain stem glioma	Midbrain
6	9	F	Brain stem glioma	Pons
7	14	M	Brain stem glioma	Pons
8	7	F	Brain stem glioma	Pons
9	13	F	Glioblastoma multiforme	Frontoparietal
10	11	M	Glioblastoma multiforme	Parietal lobe
11	17	M	Astrocytoma (low)	Temporal
12	9	M	Astrocytoma (pilocytic)	Parietal
13	12	F	Astrocytoma (pilocytic)	Thalamus
14	10	M	Spinal astrocytoma	Cervical spine (C2–C4)
15	5	M	Dysembryoplastic neuroepithelial tumor	Temporal lobe
16	5	F	Medulloblastoma	Medulla/4th ventricle
17	15	M	Craniopharyngioma	Pituitary gland
18	9	F	Optic glioma	Optic chiasm
19	17	F	Choroid plexus carcinoma	Lateral ventricle
20	8	M	Ependymoma	Medulla/4th ventricle

(mean ± SD, 1.2 ± 0.4 d). All but 3 study pairings were completed within 72 h. Several children received multiple pairs of MRI and ^{99m}Tc-MIBI scans, with 29 pairs of images being completed in total.

Imaging

Each patient was given an intravenous injection of ^{99m}Tc-MIBI at a dose calculated as body surface area divided by 1.73 and then multiplied by the adult dose of 1,000 MBq. Imaging was initiated 10–15 min later using a triple-head gamma camera (model 3000; Marconi Medical Systems, Cleveland, OH) equipped with low-energy, high-resolution collimators. The acquisition time was approximately 30 min. Reconstruction was by filtered backprojection, and images had a side thickness of 7 mm.

MR images were obtained on a 1.5-T unit with standard techniques. T1-weighted, T2-weighted, flare, and gadolinium-enhanced scans were obtained in multiple planes for all patients. These included axial, coronal, and sagittal projections that could easily be correlated with sestamibi images of the same views.

Image Analysis

^{99m}Tc-MIBI scans were analyzed and interpreted by the same nuclear medicine specialist who completed the scans. Gadolinium-enhanced MR images were analyzed by a neuroradiology specialist from the same institution. For the purposes of this study, both types of images were interpreted as either showing or not showing definitive evidence of a tumor. For cases in which repeated imaging was obtained, any evidence of an interval change from the previous set of scans was also noted. For all images, variables that were reported included tumor size, location, extent, contrast enhancement, vascular supply, and morphologic features such as solid versus cystic appearance.

Progression of tumor was determined clinically when a patient showed definitive signs of disease progression between scans. Definitive signs of progression included obvious clinical deterioration on examination or death directly attributable to the brain tumor.

RESULTS

A total of 29 pairs of MRI and ^{99m}Tc-MIBI scans from 20 children with CNS malignancy were included in the study. Age, sex, diagnosis, and tumor location are summarized in Table 1. The mean age of the children was 9.9 ± 4.4 y, and the age range was 5–17 y. This population included 12 boys and 8 girls.

A wide variety of pediatric brain neoplasms took up ^{99m}Tc-MIBI. As summarized in Table 2, these included brain stem gliomas, pilocytic astrocytoma, glioblastoma multiforme, and choroid plexus carcinoma. Tumors with no demonstrable uptake of ^{99m}Tc-MIBI when tumor was evi-

TABLE 2
Tumor Histology, Grade, and Results of ^{99m}Tc-MIBI Imaging and MRI

Patient no.	Diagnosis	Grade	^{99m}Tc-MIBI imaging	MRI
1	Brain stem glioma	I	−	++
2	Brain stem glioma	II	++	++
3	Brain stem glioma	II	++	++
	Brain stem glioma	II	++	+
	Brain stem glioma	II	++	++
	Brain stem glioma	II	++	++
4	Brain stem glioma	NA	−	+
5	Brain stem glioma	II	−	++
6	Brain stem glioma	NA	++	++
	Brain stem glioma	NA	++	++
7	Brain stem glioma	NA	++	++
8	Brain stem glioma	NA	++	++
9	Glioblastoma multiforme	IV	++	+
10	Glioblastoma multiforme	IV	−	+
	Glioblastoma multiforme	IV	++	+
	Glioblastoma multiforme	IV	−	−
11	Astrocytoma	II	−	++
12	Astrocytoma (pilocytic)	II	−	−
	Astrocytoma (pilocytic)	II	−	+
13	Astrocytoma (pilocytic)	I	++	++
14	Spinal astrocytoma	III	−	++
	Spinal astrocytoma	III	−	++
15	Desembryoplastic neuroepithelial tumor	I	−	+
16	Medulloblastoma	IV	−	++
17	Craniopharyngioma	I	−	++
18	Optic glioma	II	−	++
19	Choroid plexus carcinoma	III	++	+
	Choroid plexus carcinoma	III	−	−
20	Ependymoma	II	−	+

− = no evidence of tumor; ++ = definitive tumor; + = suggestive tumor; NA = not applicable.

dent on MRI included optic glioma, medulloblastoma, desmoplastic neuroepithelial tumor, craniopharyngioma, spinal anaplastic astrocytoma, low-grade astrocytoma, and ependymoma. Therefore, of the 29 sestamibi studies completed, 13 were true-positive, 13 were false-negative, and 3 were true-negative when positive MRI findings were used as definitive evidence of tumor. A false-negative result indicated either that no significant amount of radiotracer was taken up by the tumor or that the radiotracer had subsequently been expelled from the tumor at the time of imaging. In no instance was a positive ^{99m}Tc-MIBI result accompanied by a negative MRI result.

An example of a positive sestamibi scan is shown in Figure 1, which depicts both the gadolinium-enhanced T1- and T2-weighted MR images and the ^{99m}Tc-MIBI SPECT images for patient 9, a 13-y-old girl with a glioblastoma multiforme tumor of the right frontotemporal region. In this patient, a close morphologic correlation was observed between the positive ^{99m}Tc-MIBI image and both MR images. MR and SPECT images of a brain stem glioma can be seen in Figure 2.

Astrocytomas constituted the largest proportion of tumors in this group of children (23 pairs of scans from 15 children). Uptake of sestamibi appeared to depend in part on the histologic grade of the tumor. Of the 9 patients with intracranial astrocytomas for which histologic grading was available, 4 failed to demonstrate any positive sestamibi scans. In all of these cases, tumors were of grade I or II. Conversely, both patients with grade IV astrocytomas had positive sestamibi scans. Furthermore, of the remaining 7 nonastrocytoma tumors, the only positive sestamibi scans were in a patient with a high-grade (III) choroid plexus carcinoma.

Brain stem gliomas were the most consistently positive type of tumor in our limited sample, with 5 of 8 cases demonstrating uptake of the sestamibi tracer. All 3 of the brain stem gliomas that had negative sestamibi scans were located in the midbrain.

Normal cranial structures found to take up ^{99m}Tc-MIBI in this group of patients included the choroid plexus and the pituitary gland. In none of the 20 tumors imaged did this uptake by normal tissues interfere with the interpretation of the scan. Only 1 case of spinal cord tumor was included, and it failed to show up on SPECT despite its high grade.

Multiple pairs of MR and ^{99m}Tc-MIBI images were available for 6 children. A summary of the respective changes in both modes of imaging, the time course of these changes, and the progression or nonprogression of their illness is included in Table 3. In 2 of these 6 patients, sestamibi images remained negative at all times. In the remaining 4 patients, sestamibi activity was found to correlate well with changes found on MRI over the same period. Furthermore, in patient 3, increased tumor was noted on 2 consecutive sestamibi scans when MRI done at the same time revealed no interval change. On the final pairing for this patient, this trend was reversed: Increased tumor was noted on MRI, whereas the sestamibi scan showed decreased tumor. This progression is illustrated in Figure 2, which shows pairings of MR and SPECT images from time zero through 8, 12, and 16 mo, respectively. Throughout these changes, clinical evidence of disease progression was not seen until a few days before this child died. Therefore, the sestamibi scan was the first to show tumor progression, followed by MRI and finally by clinical signs.

DISCUSSION

Our results demonstrate the potential of ^{99m}Tc-MIBI to image many pediatric brain tumors. A positive SPECT scan using this tracer appears to depend in part on tumor histology, including both the type and the histologic grade of the

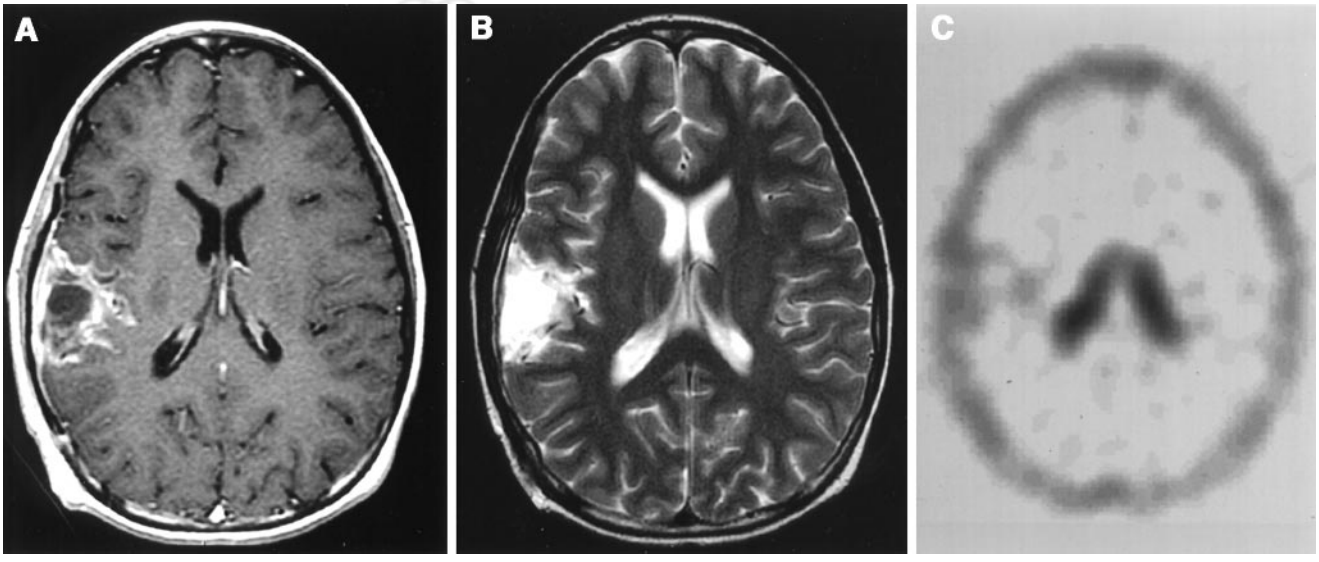

FIGURE 1. Glioblastoma multiforme of right frontotemporal region, revealed on T1-weighted MRI with gadolinium (A) and T2-weighted MRI (B), is also well defined on sestamibi scan (C).

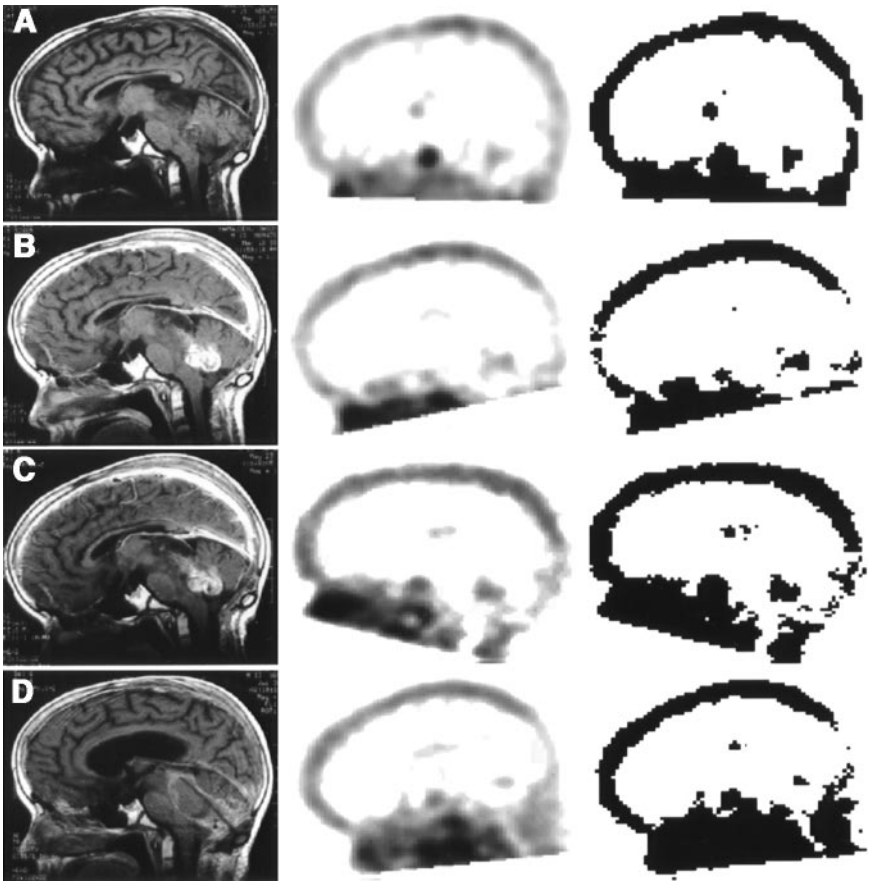

FIGURE 2. Serial pairings of sagittal MRI and SPECT images for 15-y-old boy with exophytic brain stem glioma. Third column is black-and-white version of original SPECT images. Baseline images (A) are compared with scans at 8 (B) and 12 (C) mo, both of which show increased signal on ^{99m}Tc-MIBI SPECT but no change on MRI. Final panel (D) demonstrates increased tumor on MRI at 16 mo, accompanied by decreased signal from SPECT.

tumor. Although MRI appears to be superior in many cases, the lack of consistent correlation that we observed between MRI and SPECT suggests that unique information may be available from each mode of imaging.

TABLE 3
Chronologic Changes in ^{99m}Tc-MIBI and MRI Results

Patient no.	Time (mo)	^{99m}Tc-MIBI	MRI	Progression
3	0	+	+	
	8	+I	+NC	No
	12	+I	+NC	No
	16	+D	+I	No
10	0	−	+	
	3	+	+NC	No
	6	−	−	Yes
14	0	−	+	
	6	−	+NC	Yes
6	0	+	+	
	6	+I	+I	Yes
12	0	−	−	
	14	−	+	Yes
19	0	+	+	
	16	−	−	No

+ = tumor evident; +I = increased tumor from previous image; +NC = no change in tumor from previous image; +D = decreased tumor from previous image; − = no evidence of tumor.

^{99m}Tc-MIBI is established as a marker of CNS malignancy (*2,11,14,16,24–27*), but further data are necessary to clarify the role in specific tumor types and the clinical value when these patients are followed over time. In our series, 9 of 20 lesions were positive, including both low-grade and high-grade astrocytic tumors. This finding is consistent with adult data showing positivity for multiple tumor types, including astrocytoma (*11,20*) and meningioma (*11,13,22*). However, in our study group, 11 of 20 tumors evident on MRI were not evident on SPECT. Those diagnoses included craniopharyngioma, ependymoma, desmoplastic neuroepithelial tumor, medulloblastoma, and some low-grade gliomas. This finding suggests a selectivity in tracer uptake or extrusion, which might be due to several factors. Regional blood flow, blood–brain barrier (BBB) permeability, tumor cell membrane adenosine triphosphatase pump, and mitochondrial content may influence uptake of radiotracers (*5*). Tracer needs to reach the tumor cells first through the bloodstream, and a correlation between cerebral blood flow and ^{99m}Tc-MIBI reactivity has been shown previously (*27*). The tracer must then leave the vascular lumen and cross the BBB. The inability of ^{99m}Tc-MIBI to enhance normal structures within the brain aside from the choroid plexus supports the importance BBB integrity.

In addition to being sealed by tight junctions, BBB endothelial cells also express the multidrug resistance 1 gene, the product of which is an adenosine triphosphatase mem-

brane pump extruding a variety of toxins from the cells. ^{99m}Tc-MIBI is one of these substrates (*16*). Inhibition of multidrug resistance has been shown to delay excretion of ^{99m}Tc-MIBI (*28*). Without inhibition, the pump prevents the tracer from reaching the interstitial space. Choroid plexus tissue, the vasculature of which expresses neither tight junctions nor multidrug resistance 1, accumulates ^{99m}Tc-MIBI, supporting this concept. Consequently, tumors arising from this tissue are ^{99m}Tc-MIBI positive as well (*14*).

The next barrier that the tracer must pass to enter tumor cells is the cell membrane. Passage through the cell membrane may be influenced by several factors, including multidrug resistance, mentioned above. In addition, both regional blood flow distribution and mitochondrial oxidation capacity correlated well with ^{99m}Tc-MIBI uptake in cardiac myocytes (*29*,*30*). Intracellular parameters may also determine ^{99m}Tc-MIBI accumulation, which occurs in both mitochondria and cytosol, as well as in association with specific cellular proteins (*31*). In tumor cell lines, most ^{99m}Tc-MIBI has been demonstrated to associate with the mitochondria (*32*). Therefore, metabolically active and highly malignant tumors may be more strongly positive than are lower-grade tumors. Our finding of no positivity in craniopharyngioma and some low-grade tumors, combined with well-established positivity in high-grade glioma, fits this picture. However, other investigators have also demonstrated negativity in ependymoma and medulloblastoma (*26*), tumors that are both well vascularized and metabolically active, suggesting that the answer lies beyond tumor grade alone.

Similarly, the variable results we observed in low-grade gliomas, only half of which were positive for tracer uptake, merit further investigation. These tumors are frequently located in sites where complete surgical resection is difficult, such as the optic chiasm, basal ganglia, or brain stem. The biologic behavior of brain tumors remains difficult to predict by histology alone, and the success of nonsurgical treatments is limited. Therefore, clarifying the nature of the variability of SPECT findings in pediatric low-grade glioma has the potential to add a clinically valuable piece of information to allow a more accurate prediction of clinical behavior over time.

The effect of previous surgery, radiation, or chemotherapy on ^{99m}Tc-MIBI uptake is poorly established in the literature. In pediatric brain tumors, the progression of tumor at the edge of a previously resected site may be preferentially imaged by ^{99m}Tc-MIBI as opposed to ^{201}Tl (*2*). Isolated case reports suggest that the ^{99m}Tc-MIBI signal is decreased in tumor cells after radiation treatment (*27*,*33*). Decreased SPECT activity after therapy despite no change in tumor size by CT or MRI has been shown (*27*), suggesting that such imaging may be a more sensitive measure of response to treatment. Our results from 6 patients for whom consecutive pairs of images were available are insufficient to significantly support an advantage of sestamibi scans. However, in 1 patient with high-grade glioma, progression on ^{99m}Tc-MIBI appeared to precede any evidence of progression on MRI or clinically. Therefore, similarities in the information available from SPECT may exist between adult and pediatric patients with brain tumors.

CONCLUSION

Our results demonstrate the potential uses of ^{99m}Tc-MIBI SPECT in the imaging of astrocytic pediatric brain malignancy. We suggest that larger studies be undertaken to better assess the clinical utility of this tool, particularly in low-grade gliomas of childhood.

REFERENCES

1. Oriuchi N, Tamura M, Shibazaki T, Ohye C, Watanabe N. Clinical evaluation of thallium-201 SPECT in supratentorial gliomas: relationship to histological grade, prognosis, and proliferative activities. *J Nucl Med.* 1993;34:2089–2090.
2. O'Tuama LA, Treves ST, Larar JN. Thallium-201 versus technetium-99m-MIBI SPECT in evaluation of childhood brain tumors: a within subject comparison. *J Nucl Med.* 1993;34:1045–1051.
3. Bahargava S, Coel M, Wilkinson R. Thallium-201 single photon emission computed tomography imaging in a pediatric brain tumor: a case report. *Pediatr Neurosurg.* 1991;17:95–97.
4. Carvalho PA, Schwartz RB, Alexander E. Extracranial metastatic glioblastoma: appearance on thallium-201-chloride/technetium-99m-HMPAO SPECT images. *J Nucl Med.* 1991;32:322–324.
5. Kaplan WD, Takvorian T, Morris JH, et al. Thallium-201 brain tumor imaging: a comparative study with pathologic correlation. *J Nucl Med.* 1987;28:47–57.
6. Black RL, Hawkis RA, Kim KT. Use of thallium-201 SPECT to quantitate malignancy grade of gliomas. *J Neurosurg.* 1989;71:342–346.
7. Kim KT, Black KT, Marciano D. Thallium-201 SPECT imaging of brain tumors: methods and results. *J Nucl Med.* 1990;31:965–969.
8. Schwatrz RB, Carvalho PA, Alexander E, Loeffler JS, Folkerth R, Holman BL. Radiation necrosis versus high-grade recurrent glioma: differentiation by using dual-isotope SPECT with ^{201}Tl and ^{99m}Tc-HMPAO. *AJNR.* 1992;12:1187–1192.
9. O'Tuama LA, Janicek MJ, Barnes PD, et al. ^{201}Tl/^{99m}Tc-HMPAO SPECT imaging of treated childhood brain tumors. *Pediatr Neurol.* 1991;7:249–257.
10. Rollins N, Lowry P, Shapiro K. Comparison of gadolinium enhanced MR and thallium-201 single photon emission computed tomography in pediatric brain tumors. *Pediatr Neurosurg.* 1995;22:8–14.
11. Bagni B, Pinna L, Tamarozzi R, et al. SPET imaging of intracranial tumours with 99Tcm-sestamibi. *Nucl Med Commun.* 1995;16:258–264.
12. Aktolun C, Bayhan H, Kir M. Clinical experience with Tc-99m MIBI imaging in patients with malignant tumors: preliminary results and comparison with Tl-201. *Clin Nucl Med.* 1992;17:171–176.
13. Park CH, Sataloff R, Richard M, Zhang M, Kim SM. Tc-99m MIBI brain SPECT of cerebellopontine angle tumors. *Clin Nucl Med.* 1996;21:375–378.
14. Wolff JEA, Myles T, Egeler M, Pinto A, Kloiber T. Sestamibi detection of choroid plexus carcinoma. *Med Pediatr Oncol.* 2000;25:401–409.
15. Balon HR, Fink-Bennet TD, Stoffer SS. Technetium-99m-sestamibi uptake by recurrent Hurthle cell carcinoma of the thyroid. *J Nucl Med.* 1992;33:1393–1395.
16. Yokogami K, Kawano H, Moriyama T, et al. Application of SPET using technetium-99m sestamibi in brain tumours and comparison with expression of the MDR-1 gene: is it possible to predict the response to chemotherapy in patients with gliomas by means of ^{99m}Tc-sestamibi SPET? *Eur J Nucl Med.* 1998;25:401–409.
17. Maublant JC, Zhang Z, Rapp M, Ollier M, Michelot J, Veyre A. In vitro uptake of technetium-99m-teboroxime in carcinoma cell lines and normal cells: comparison with technetium-99m-sestamibi and thallium-201. *J Nucl Med.* 1993;34:1949–1952.
18. Briele B, Hotze A, Kropp J, et al. Comparison of 201-thallium and 99m-Tc-MIBI in the follow-up of undifferentiated thyroid carcinoma. *Nuklearmedizin.* 1991;30:115–124.
19. Caner B, Kitapci M, Aras T, et al. Increased accumulation of hexakis (2-methoxyisobutylisonitrile) technetium in osteosarcoma and its metastatic lymph nodes. *J Nucl Med.* 1991;32:1977–1978.
20. Baillet G, Albequerque L, Chen Q, Poisson M, Delattre JY. Evaluation of single photon emission tomography imaging of supratentorial brain gliomas with technetium-99m-sestamibi. *Eur J Nucl Med.* 1994;21:1061–1066.

21. Park CH, Kim SM, Zhang JJ, Intenzo CM, McEwan JR. Tc-99m MIBI brain SPECT in the diagnosis of recurrent glioma. *Clin Nucl Med.* 1994;19:57–58.
22. Shih WJ, Lee JK, Milan P. Discordant technetium-99m-MIBI and technetium-99m-HMPAO uptake of recurrent occipital meningioma on brain SPECT images. *J Nucl Med.* 1996;37:1183–1185.
23. Mira ML, Popa N, Huysmans E, Lenaers A, Schoutens A. Tc-99m sestamibi SPECT imaging of a brain metastasis in a man with lung tumor and increased sexual activity. *Clin Nucl Med.* 1996;21:745–746.
24. Maffioli L, Gasparini M, Chiti A, et al. Clinical role of technetium-99m sestamibi single photon emission tomography in evaluating pretreated patients with brain tumors. *Eur J Nucl Med.* 1996;23:308–311.
25. O'Tuama LA, Packard AB, Treves ST. SPECT imaging of pediatric brain tumors with hexakis (methoxyisobutylisonitrile) technetium. *J Nucl Med.* 1990; 31:2040–2041.
26. Arbab AS, Koizumi K, Toyama K, Araki T. Uptake of technetium-99m-tetrofosmin, technetium-99m-sestamibi, and thallium-201 in tumor cell lines. *J Nucl Med.* 1996;37:1551–1556.
27. Tomura N, Hirano H, Watanabe O, et al. Preliminary results with technetium-99m MIBI SPECT imaging in patients with brain tumors: correlation with histological and neuroradiological diagnoses and therapeutic response. *Comput Med Imaging Graph.* 1997;21:293–298.
28. Luker GD, Fracasso PM, Dobkin J, Piwnica-Worms D. Modulation of the multidrug resistance P-glycoprotein: detection with technetium-99m-sestamibi in vivo. *J Nucl Med.* 1997;38:369–372.
29. Mountz JM, Raymond PA, McKeever PE. Specific localization of thallium-201 in human high-grade astrocytoma by microautoradiography. *Cancer Res.* 1989; 49:4053–4057.
30. Crane P, Laliberte R, Heminway S. Effect of mitochondrial viability and metabolism of technetium-99m-sestamibi. *Eur J Nucl Med.* 1993;20:20–25.
31. Delmon-Moingeon LI, Piwnica-Worms D, van den Abbeele, et al. Uptake of the cation hexakis (2-methoxyisobutylisonitrile)-technetium-99m by human carcinoma cell lines in vitro. *Cancer Res.* 1990;50:2198–2202.
32. O'Tuama LA, Poussaint TY, Anthony DC, Treves ST. Childhood brain tumor: neuroimaging correlated with disease outcome. *Pediatr Neurol.* 1998;19:259–262.
33. Hassan IM, Sahweil A, Constantinides C, et al. Uptake and kinetics of Tc-99m hexakis 2-methoxy isobutylisonitrile in benign and malignant lesions of the lungs. *Clin Nucl Med.* 1989;14:333–340.